INTERNATIONAL JOURNAL OF HYDROGEN ENERGY 41 (2016) 1120–1133

Available online at www.sciencedirect.com

ScienceDirect

journal homepage: www.elsevier.com/locate/he

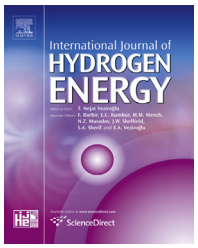

Study on the effect of the degree of grafting on the performance of polyethylene-based anion exchange membrane for fuel cell application

Richard Espiritu [a,b,*], *Mohamed Mamlouk* [a], *Keith Scott* [a]

[a] *School of Chemical Engineering and Advanced Materials, Newcastle University, Merz Court, Newcastle upon Tyne, NE1 7RU, United Kingdom*

[b] *Department of Mining, Metallurgical and Materials Engineering, University of the Philippines Diliman, Quezon City 1101, Philippines*

ARTICLE INFO

Article history:
Received 15 July 2015
Received in revised form
25 September 2015
Accepted 24 October 2015
Available online 12 November 2015

Keywords:
Polyethylene
Degree of grafting
Anion exchange membrane
Radiation grafting
Alkaline fuel cell

ABSTRACT

Alkaline anion exchange membranes (AAEM) are fabricated using polyethylene as the base polymer offering a low cost AAEM. This study focuses on the synthesis and characterisation of AAEM with controlled degree of grafting (DOG) and ion-exchange capacity (IEC) with the following parameters investigated: LDPE film thickness 30–130 μm, gamma radiation dose and monomer concentration. The corresponding IEC, water uptake (WU) and degree of swelling (DS) are reported. The performance of 74.6% DOG membrane in a hydrogen fuel cell shows high OCV of 1.06 V with peak power density of 608 mW cm^{-2} at 50 °C under oxygen. The use of membrane with high DOG does not impact fuel cross-over significantly and provides improved fuel cell performance due to better conductivity, water transport and resilience to dehydration. The AAEM shows long term stability at 80 °C exhibiting a conductivity of ca. 0.11 S cm^{-1} over a period of 7 months under nitrogen. The membrane shows a degradation rate of 4 and 17 mS $month^{-1}$ under nitrogen and oxygen, respectively. The estimated life time of the membrane is 2 years under nitrogen and 5.5 months under oxygen operating at 80 °C.

Introduction

Renewed interest in the research and development of alkaline fuel cells has grown recently with the use of anion-exchange membrane (AEM) instead of liquid KOH as the electrolyte. An AEM is a solid polymer electrolyte membrane that contains positive ionic groups, typically containing quaternary ammonium groups: $-N^{+}CH_3$, and mobile negatively charged anions, usually OH^{-} [1]. The alkaline anion-exchange membrane fuel cell (AAEMFC) has been developed to address the challenges and limitations of the conventional AFCs. The AAEMFC offers the following advantages compared to proton-exchange membrane fuel cells (PEMFC), namely, (a) faster oxygen reduction reaction (ORR) kinetics under alkaline conditions, thus providing lower activation losses [2,3], (b)

* *Corresponding author*. School of Chemical Engineering and Advanced Materials, Newcastle University, Merz Court, Newcastle upon Tyne, NE1 7RU, United Kingdom.
E-mail address: r.espiritu@newcastle.ac.uk (R. Espiritu).

http://dx.doi.org/10.1016/j.ijhydene.2015.10.108

possibility of using non-noble metal catalysts [4–6], (c) osmotic drag associated with ion transport opposes the crossover of liquid fuels [4,7] and (d) lower membrane cost and cheaper cell components due to less corrosive environments [2,5,7].

The materials and methods required to produce AEMs are influenced by the desired properties of the resulting membrane in terms of performance, durability, stability and cost. The chemical and thermal stability greatly depend on the nature of the polymer backbone and on the functional group that enables the transfer of hydroxyl ions [8]. With these in mind, the major challenge is to synthesise AEM with a high OH^- ion conductivity using a stable polymer backbone with high ion exchange capacity but with controlled swelling and water uptake. One way to address this challenge is by employing polymer modification via grafting technique [9].

Radiation grafting is a widely used technique in industrial applications in order to improve the properties of the resulting polymer product [10] without altering their individual inherent properties [11]. In this method, active sites are formed on the polymer backbone using high energy radiation (gamma radiation, ultraviolet or electrons) and the irradiated base polymer is allowed to react with the monomer units which then propagate to form side chain grafts [9]. In fuel cell technology applications, in particular, radiation grafting is a cheaper way of producing ionomer membranes and offers a wealth of adjustable experimental parameters (e.g. radiation dose, temperature, film thickness) thus providing a large degree of tailorability [6]. Furthermore, reaction is completed in a fraction of a second, thus high product yield is obtained [12]. In terms of fuel cell performance, AEMs produced via radiation grafting can have high degree of grafting (DOG), low electrolytic resistivity, high IEC and high equilibrium water content [13].

The measure of the extent of polymerisation is often expressed in terms of the DOG. It is defined as the percentage mass of the grafted component with the copolymer matrix [14] and is an important parameter routinely studied due to its significant influence on the resulting properties of the AEM, namely, IEC, ionic conductivity, water uptake and swelling. In employing radiation to induce grafting of monomers, the type of radiation source, radiation dose and dose rate are important considerations that affect the resulting DOG of the membrane [15].

Polyethylene has been found to be a lucrative polymer backbone for AEMs due to its low cost, superior chemical stability, high crystallinity and hydrophobicity, good mechanical properties [16,17] and versatility to radiation grafting both for electrolyser and fuel cell applications [14,15,18]. Masson et al. [19] utilised gamma radiation source to graft low density polyethylene (LDPE) with acrylic acid followed by sulfonation while Faraj et al. [20] utilised UV-radiation source to graft LDPE with vinylbenzyl chloride (VBC) with subsequent amination to fabricate AEMs for water electrolysis. In terms of fuel cell application, Mamlouk et al. [21,22] successfully fabricated AEMs for alkaline fuel cells using LDPE and high density polyethylene (HDPE) as base polymer and employing VBC as the graft monomer. Aside from LDPE and HDPE based membranes for alkaline fuel cells, ultrahigh molecular weight polyethylene (UHMWPE) has also been used for radiation grafting but requires a melt pressing method to produce the membrane [23]. Shen et al. [24] on the other hand, performed methanol permeation studies on LDPE-based AEM for direct methanol fuel cells while Cheng et al. [25] evaluated the performance of LDPE-based AEM for direct borohydride fuel cell application.

Evolving research trend on polyethylene-based membranes involves grafting of polyethylene with another polymer in order to obtain the desired chemical and mechanical properties of the resulting copolymer backbone prior to functionalisation. Kim et al. [17] exploited the innate hydrophobicity of polyethylene and chemically grafted it with sulfonated poly(arylene ether sulfone) to produce membranes with high ion exchange capacity but with controlled swelling and water uptake. The work of Noonan et al. [26] showed the preparation of membranes with superb alkaline stability by chemically attaching phosphonium-based functional groups to polyethylene. Moreover, pore-filled composite membranes based on porous polyethylene exhibited high durability [27] and enhanced mechanical stability for high temperature fuel cell operation [28].

This particular study focuses on the facile synthesis and subsequent characterisation of AEM for alkaline fuel cells using LDPE alone as the base polymer thus offering an essentially cheaper alternative than commercially available AAEM. The effect of the DOG on the ionic conductivity and fuel cell performance, as influenced by gamma radiation dose and monomer concentration, is hereby investigated. Furthermore, this research examined the stability of the fabricated membranes in the vapour phase operating condition, which previous reports in literature have not included.

Experimental

Materials

Low-density polyethylene (melt index of 25 g/10 min) and linear low-density polyethylene (melt index of 1 g/10 min) pellets were procured from Sigma–Aldrich. Commercial polyethylene films were sourced from different suppliers, namely, British Polythene Industries plc (BPI) and VWR International (VWR). Microporous ultra-high molecular weight polyethylene (UHMWPE) films, with 40% porosity, were purchased from Entek Membrane LLC (ENTEK, USA). Vinylbenzyl chloride (mixture of 3– and 4–isomers, 97%) and trimethyl amine (in 45% solution in H_2O) were also procured from Sigma–Aldrich. Toluene solvent, potassium hydroxide pellets, acetone, methanol, sulphuric acid and sodium chloride were all analytical reagent grade and were used as received.

Anion exchange membrane preparation

Anion-exchange membranes (AEM) were synthesised using polyethylene as base polymer followed by radiation grafting with vinylbenzyl chloride (VBC) to form the copolymer. To obtain the AEM, trimethyl amine (TMA) was used to impart functionality to the copolymer. Aside from using commercial polyethylene films as base polymer, laboratory-produced polyethylene films were also prepared from commercial pellets and cast them into films.

Casting of polyethylene films

Pre-calculated amounts of low-density polyethylene (LDPE) and linear low-density polyethylene (LLDPE) were dissolved in 30 mL toluene solvent to obtain solutions of 5% by weight and 2% by weight of LDPE and LLDPE, respectively. Dissolution of polyethylene was performed by heating with agitation. After complete dissolution of polymer in hot toluene, appropriate amounts of 5% LDPE and 2% LLDPE were extracted using a syringe and were transferred to a pre-heated Petri dish placed inside a metal chamber submerged in a Grant GD120 hot water bath set to 90 °C. Toluene solvent was allowed to completely evaporate to produce the membrane films.

Heat treatment of cast polyethylene films

In order to obtain strong polyethylene films and to completely remove trapped solvent, cast membranes were subjected to heat treatment. LDPE-cast membranes were placed inside the Lenton ECF 12/30 furnace at 130 °C while the temperature setting for LLDPE-cast membranes was 150 °C. Polyethylene samples were heat-treated for 30 min and were allowed to cool to room temperature inside the furnace. Afterwhich, polyethylene films were then peeled from the Petri dish.

Radiation grafting of polyethylene films

Fig. 1 shows the schematic of the preparation of LDPE-based AAEM. Both commercially procured and as-cast polyethylene films of a constant thickness of 50 μm, were cut in to 4 cm × 8 cm dimension. The films were washed with acetone and allowed to dry. Two samples of each polyethylene film were prepared and their initial weights were recorded. They were then subsequently placed inside a screw-cap vial. VBC monomer was added to each vial in the following concentrations: 10/36/54 and 31/26/45 by volume VBC/toluene/methanol, respectively. Samples were then sent to Synergy Health plc (Wiltshire, UK) for gamma radiation treatment. The samples were subjected to gamma radiation with total dose of

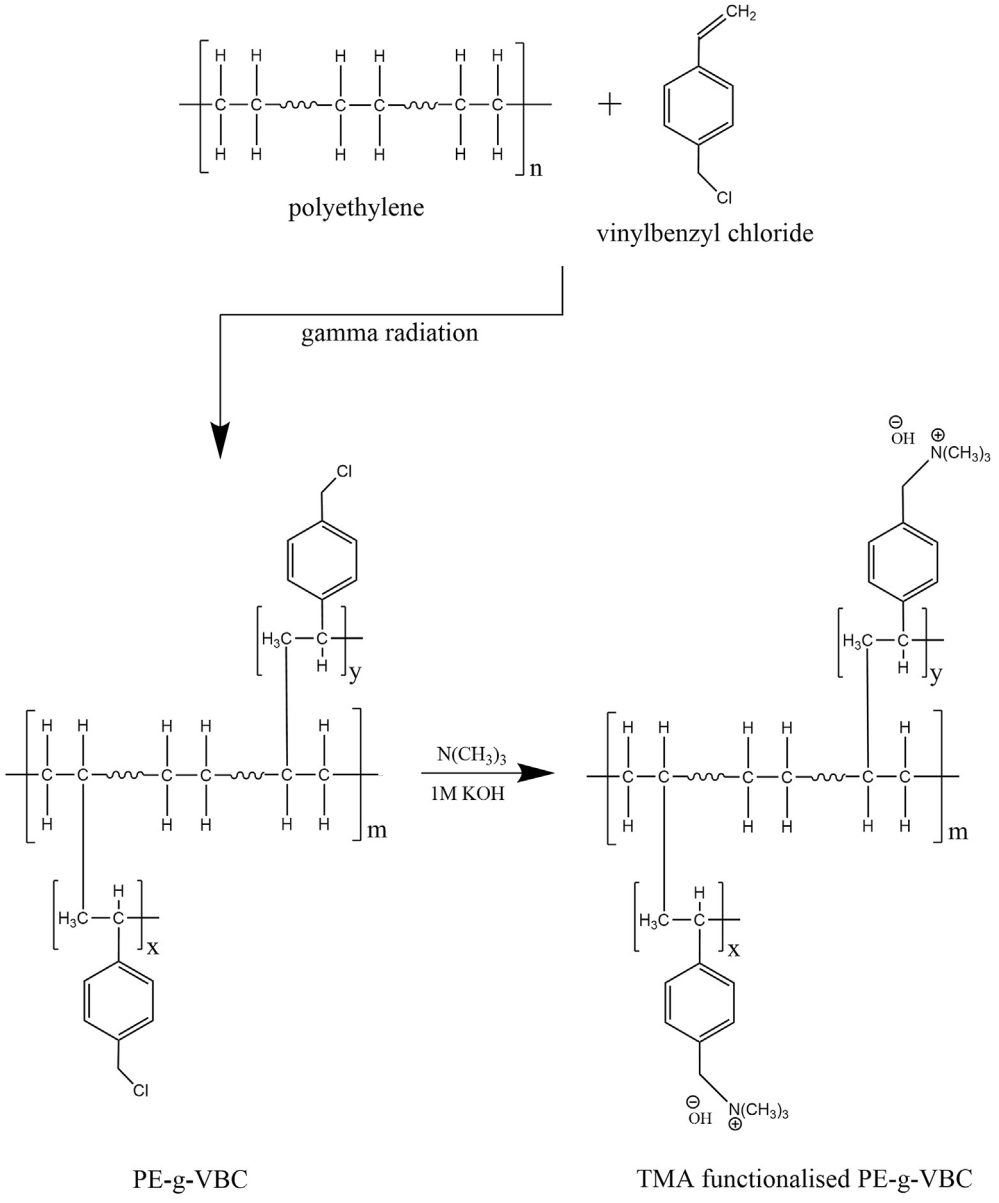

Fig. 1 – Schematic of synthesis of polyethylene based AAEM.

10 kGy and 20 kGy at dose rate of 2.0 kGy h^{-1}. Radiation grafted membranes were then washed with toluene, then with acetone and were subsequently ultrasonicated for 5 min. The membranes were allowed to dry and the final weights were recorded. To investigate the effect of varying the initial polyethylene thickness, another set of polyethylene films with thicknesses of 30, 50, 75 and 130 μm were prepared and were subjected to the same radiation grafting.

Functionalisation of the membranes

A previous study [29] revealed that, from a selection of various amines and sulfide functional groups investigated, TMA functionalised membranes offered the highest conductivity and superior fuel cell performance in comparison to other functional groups. Therefore, TMA was used to functionalise each PE-g-VBC membrane sample (Fig. 1) and allowed to soak for sufficient amount of time. The membranes were then washed repeatedly with deionised water.

Characterisation of AEMs

Degree of grafting

The degree of grafting (DOG) of the membrane was measured from the weights of the membrane before and after gamma irradiation using the following formula:

$$DOG(\%) = \frac{W_a - W_o}{W_a} \times 100 \quad (1)$$

where W_a is the weight of the polymer after irradiation and W_o is the weight of the polymer before irradiation.

Fourier-transform infrared (FTIR) spectroscopy

Verification of chemical structure and presence of functional groups were performed using Varian 800 FT-IR Spectrometer at scan range of 3800 to 600 cm^{-1} equipped with Pike Technologies diamond crystal plate Attenuated Total Reflectance (ATR) unit. Samples of original polyethylene, VBC-grafted polyethylene and TMA-functionalised PE-g-VBC were subjected to analysis.

Measurement of ion-exchange capacity

The ion-exchange capacity (IEC) of each membrane was measured using acid-base titration. Membranes were treated with fresh 1.0 M KOH solution every 20 min for three times (total OH^- exchange time of 1 h) to completely exchange the chloride ions with hydroxide ions. The membrane was then washed with copious amount of deionised water to remove residual hydroxide ions. Removal of excess OH^- ions was confirmed by using pH paper. The membrane was subsequently immersed in a known volume of 1.0 M NaCl and was let to stand overnight. The liberated hydroxide ions were then titrated with 0.05 M H_2SO_4 using Brand GMBH Titrette bottle-top burette and the endpoint was determined visually using methyl red indicator. The membrane was thoroughly washed with deionised water to remove excess salt and was allowed to dry. The IEC was computed using the amount of OH^- ions neutralised, expressed in mmol divided by the dry weight of the membrane, in grams. The measured IEC was then compared to the theoretical IEC, computed as shown in equation below which assumes complete amination, ion-exchange and full removal of water upon drying.

$$IEC_{theo}\left(mmol g^{-1}\right) = \frac{1000 \times \frac{\left(W_{LDPE-g-VBC} - W_{LDPE}\right)}{MW_{VBC}}}{W_{LDPE-g-VBC} + \frac{\left(W_{LDPE-g-VBC} - W_{LDPE}\right)}{MW_{VBC}} \times MW_{TMA}} \quad (2)$$

where $W_{LDPE\text{-}g\text{-}VBC}$ and W_{LDPE} are the weights of the grafted membrane and initial LDPE respectively; and MW_{VBC} and MW_{TMA} are molecular weights of VBC and TMA, respectively.

Water uptake, hydration number and swelling measurement

Water uptake (WU) was determined from the difference in weights between the hydrated and the dried polymer membrane. OH^- exchanged membranes were immersed in deionised water at room temperature. After 48 h, wet membranes were collected and pat dry with tissue paper to remove surface water. The thickness, dimensions and weight of the hydrated membrane were subsequently measured. To obtain the weight of the dry membrane, the hydrated membranes were oven-dried at 60 °C and weighed repeatedly until a constant weight and dimensions were obtained. The WU, in terms of wt %, was computed as follows:

$$WU(wt\%) = \frac{W_{wet} - W_{dry}}{W_{dry}} \times 100 \quad (3)$$

where W_{wet} and W_{dry} were the wet and dry weights of the membrane, respectively. Consequently, the volumetric WU was determined taking into consideration the density of the polymer and with the assumption that the total volume is simply the sum of volume of the water phase and the polymer phase of the swollen membrane (Equation (4)) [30].

$$WU(vol\%) = \frac{\frac{\left(W_{wet} - W_{dry}\right)}{\rho_{water}}}{\frac{\left(W_{wet} - W_{dry}\right)}{\rho_{water}} + \frac{W_{dry}}{\rho_{polymer}}} \times 100 \quad (4)$$

where ρ_{water} and $\rho_{polymer}$ are the densities of water (1 g cm^{-3}) and the grafted and functionalised polymer (0.95 g cm^{-3}), respectively.

The hydration number (λ), which is the number of water molecules per trimethyl amine group, was calculated using the IEC and the gravimetric WU data as shown below:

$$\lambda = \frac{WU(wt\%) \times 10}{MW_{water} \times IEC} \quad (5)$$

where MW_{water} is the molecular weight of water, 18.01 g mol^{-1}.

The degree of swelling (DS) was measured as the average of swelling in width, in length and in thickness, of the membrane before and after drying, as shown below:

$$DS(\%) = \frac{D_{wet} - D_{dry}}{D_{dry}} \times 100 \quad (6)$$

where D_{wet}, is the dimension, of the wet membrane in a given direction (width (x-axis), length (y-axis) or thickness (z-axis)) and D_{dry}, is the corresponding dimension of the dry membrane in a given direction.

Mechanical testing

Tensile testing of the LDPE base film, dry AEM and fully hydrated AEM of different DOG was performed. A fully hydrated Nafion 212 film was also tested for comparison. To prepare fully hydrated AEMs, membranes were soaked in deionised water for at least 48 h prior to tensile testing. A Shimadzu Autograph AGS-X Universal Testing Machine was employed to obtain the stress–strain plot applying a constant crosshead speed of 2 mm min^{-1} for all the test specimens.

Measurement of ionic conductivity

Grafted membranes were OH^- exchanged using 1.0 M KOH solution for initial 20 min. The solution was then replaced with fresh 1.0 M KOH solution and was allowed to exchange for another 20 min. The process was repeated until a total OH^- exchange time of 1 h is achieved. Afterwhich, the membranes were thoroughly washed with deionised water. Removal of excess OH^- ions was confirmed by using pH paper. Initial thickness of the membrane was measured using a Mitutuyo No. 293-240 digimatic micrometer calliper. Each membrane was then sandwiched in between two Freudenberg FCCT H2315-C2 gas diffusion layer carbon electrodes and was placed in a gold-plated titanium test cell. The environment inside the test cell was maintained at atmospheric pressure and the humidifier temperature was set to ensure 100% relative humidity inside the cell. The relative humidity inside the fuel cell was verified using a Vaisala HUMICAP humidity sensor. The through-plane conductivity was measured using two-point technique with one probe placed on either side of the membrane. The impedance was measured using N4L NumetriQ PSM 1735 Frequency Response Analyser within the frequency range of 200 kHz–20 kHz with perturbation voltage amplitude of 15 mV. Three readings of the impedance in 5 min intervals were made and the average was reported. Consequently, the conductivity of the membrane was computed based on the following formula:

$$\sigma = \frac{4L}{R(\pi d^2)} \tag{7}$$

where σ is the hydroxyl ion conductivity, L is the membrane thickness, R is the resistance derived from the impedance value at zero-phase angle and d is the diameter of the membrane test area.

Fuel cell test

Fuel cell electrodes made from catalyst inks were used for testing as previously prepared [2,21]. A titanium-made hydrogen fuel cell, with a 1 cm^2 gold-coated serpentine flow field was used. Each membrane was OH-exchanged using the same alkaline treatment. Polarisation curve of each anion exchange membrane was obtained using Autolab PGSTAT302 Potentiostat with a scan rate of 2 mV s^{-1}. The test cell was subjected to several cycle runs until stable performance is obtained at hydrogen and oxygen stoichiometry of 1.2 and air of 2.2.

Membrane stability test

VWR-based PE-g-VBC functionalised with TMA was converted to OH^- form in sealed bottles at room temperature. The membrane was washed several times with deionised water prior to conductivity measurement following the procedure stated earlier. Conductivity measurements were made at 40, 50, 60, 70 and 80 °C taking note to obtain a stable conductivity reading at each temperature regime before shifting to a higher temperature.

Results and discussion

Polyethylene film casting

One of the parameters investigated in this research is to study the influence of the variability in polyethylene films supply source onto the fabricated polyethylene-based AAEM. This is because batches of commercial polyethylene films could differ in properties like molecular weight, melting and glass transition temperature, melt index and the type and content of additives. Due to limited solubility of polyethylene in hot toluene, the highest concentrations produced were 5% and 2% by weight for LDPE and LLDPE, respectively. It was found that LDPE and LLDPE dissolved in toluene at temperatures 60 and 91 °C, respectively.

Radiation grafting of polyethylene films

The polyethylene films were placed in a vial and added with 10/36/54 and 31/26/43 by volume VBC/toluene/methanol solution adapting the procedure of Horsfall and Lovell [31] and Cheng et al. [25], with modifications. The toluene served as the solvent for the VBC while methanol was used to swell the LDPE film so that VBC monomer can more effectively penetrate the LDPE structure. They were then subjected to gamma radiation of 10 kGy and 20 kGy total dose. The results are shown in Table 1. Both the as-cast and commercial LDPE-

Table 1 – Degree of grafting for polyethylene membranes subjected to different VBC monomer concentration and gamma radiation dose.

Polyethylene source	Degree of grafting (DOG), %			
	10/36/54 by volume VBC/toluene/methanol		31/26/43 by volume VBC/toluene/methanol	
	10 kGy	20 kGy	10 kGy	20 kGy
BPI-LDPE	4.4	16.3	50.4	74.6
ENTEK-UHMWPE	21.0	46.0	57.4	83.9
VWR-LDPE	5.6	13.1	47.9	71.3
Sigma–Aldrich – Cast LDPE	7.1	21.8	52.9	69.6
Sigma–Aldrich – Cast LLDPE	1.2	13.4	48.7	70.7

based membranes grafted poorly at low VBC concentration and low gamma radiation dose. Increasing the concentration of the VBC monomer produced a marked increase in the degree of grafting (DOG). The BPI-polyethylene based membrane, in particular, showed the highest percentage increase in DOG from 16.3% to 74.6% both subjected to 20 kGy radiation dose. This is due to the presence of more monomer available (higher concentration) for grafting to the polymer backbone. It can be also observed that an increase in the total gamma radiation dose results in increase in the DOG of the membranes. This is due to the fact that more high energy radiation is supplied to cause the formation of active sites for the VBC monomer to tether to the polyethylene backbone.

ENTEK UHMWPE porous membrane showed the highest DOG for all VBC concentrations and gamma radiation doses as compared to all of the other studied non-porous PE membranes. ENTEK UHMWPE exhibited a four-fold increase in DOG from 21.0% at low VBC concentration and low gamma radiation dose to 83.9% DOG at both high VBC concentration and gamma radiation dose. At low VBC concentration and low radiation dose, ENTEK-based membrane showed three-fold higher DOG in comparison to any of the other studied membranes. This is because even at low VBC concentration, the monomer can still easily penetrate within the porous structure of the ENTEK base polymer with high mass transport rate in comparison to the non-porous films. Unfortunately, while the grafting resulted in a decrease in the porosity from the original 40%, the ENTEK-based membrane remained porous (>5%) after grafting with very high rate of hydrogen cross-over rendering it not suitable for fuel cell applications. When the concentration of the monomer was increased, the mass transport of the VBC monomer through the LDPE film became no longer a limiting factor and the observed DOG became similar to the other non-porous LDPE-based membranes.

In the case of cast-PE membranes, both the cast-LDPE and cast-LLDPE showed almost the same high value of DOG at both high VBC concentration and gamma radiation dose. At low VBC concentration however, cast-LDPE showed higher DOG than cast-LLDPE. This is attributed to the difference in the polymer architecture between LDPE and LLDPE. Due to the absence of long chain branching in LLDPE, fewer sites are available for monomer attachment, requiring higher energies and resulting in a lower DOG. Radiation grafting favours a more branched structure wherein more sites for grafting are present compared to just a fixed long chain. However, with the increase in VBC concentration and radiation dose, the difference in DOG became negligible between the two structures.

The use of low-density polyethylene films from different sources showed no effect on the observed DOG at both high VBC concentration and gamma radiation dose. Even at low monomer concentrations, similar structure LDPE-based membranes showed very minimal variation in the observed DOG. This indicates that varying the PE supplier source has minimal effect on the PE grafting.

Characterisation of the membranes by FTIR analysis

The chemical structures of polyethylene, PE-g-VBC and functionalised PE-g-VBC were analysed by FTIR analysis, as shown in Fig. 2. The polyethylene spectra (i), being predominantly composed of methylene groups, is characterised by the presence of methylene stretches and bends. The spectra revealed four sharp peaks, namely the $-CH_2$ asymmetric stretching at 2916 cm^{-1} (■) and symmetry stretching at 2849 cm^{-1} (*) and $-CH_2$ deformation (stretching and bending) at 1463 cm^{-1} (●) and 719 cm^{-1} (□) [32]. Comparison between the non-irradiated and the irradiated polyethylene film as shown in (ii) revealed presence of only the same dominant bands indicating that no structural damage to the polymer backbone was observed after gamma irradiation [33]. This is because the radiation dose of 20 kGy was not high enough to cause significant damage to the polyethylene structure [34,35].

The VBC-grafted polyethylene (ii) showed additional peaks attributed to the presence of chlorobenzyl functional group. The stretching of C=C aromatic double bonds was observed at peaks between 1400 cm^{-1} to 1600 cm^{-1} (Δ). Bands observed at

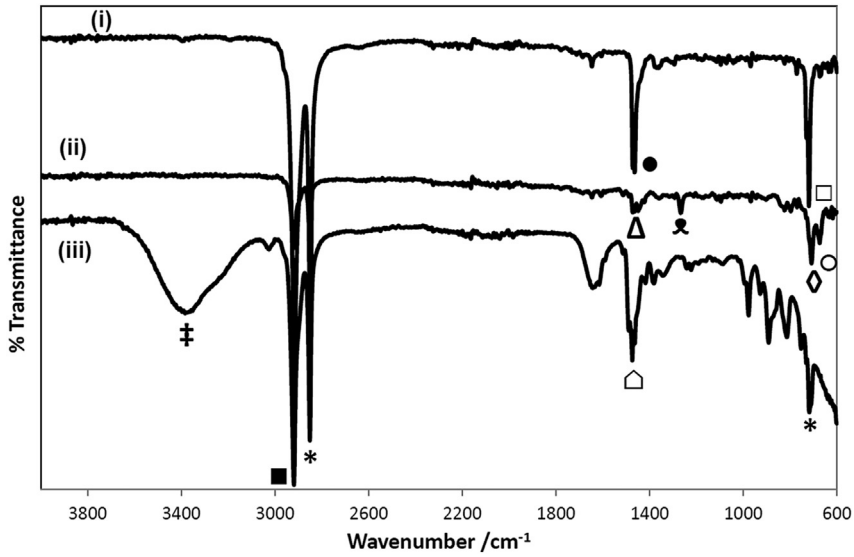

Fig. 2 – FTIR Spectra of (i) original polyethylene, (ii) VWR-based PE-g-VBC and (iii) functionalised PE-g-VBC.

Table 2 – IEC of membranes with different polyethylene sources with the same initial thickness of 50 μm.

Polyethylene source	DOG (%)	IEC (mmol g^{-1})
ENTEK (USA)	46.0	2.0
	57.4	2.5
VWR (UK)	51.7	2.3
	71.3	3.0
Sigma–Aldrich (Cast LLDPE)	70.7	2.9
BPI (UK)	50.4	2.4
	74.6	3.2

823 cm^{-1}, 796 cm^{-1} and 708 cm^{-1} (◊) were consistent with the meta and/or para benzene ring substitution of the VBC. Furthermore, the C–Cl stretching was observed at 673 cm^{-1} (○) and CH_2–Cl wagging band at 1266 cm^{-1} (♀) [36].

The spectra of TMA-functionalised PE-g-VBC (iii) exhibited additional peaks, particularly at 3377 cm^{-1} (‡) which can be attributed to –OH stretching from the residual water present in the membrane. The band at 1474 cm^{-1} (♤) can be attributed to symmetric N–CH_3 deformation. Also, it can be observed that the CH_2–Cl wagging band and the C–Cl stretching peak both observed in (ii) were no longer present, confirming the release of Cl^- and bonding with N^+ upon successful quaternisation [20].

IEC, membrane swelling and WU

Representative samples of grafted membranes were subjected to IEC measurement, by measuring the amount of OH^- ions released by exchanging it with Cl^- ions employing acid-base titration. IEC is the measure of the number of functional groups available for OH^- ion exchange per weight of dry membrane.

Table 2 shows the computed IEC in relation to the corresponding DOG for the prepared membrane from different polymer sources. The IEC increased with increasing DOG, as more functional groups were attached to the polymer backbone and more sites available for OH^- ion exchange.

Table 3 shows the effect of increasing the initial polyethylene thickness on the IEC and DOG of the produced membrane. The use of varying initial thickness of polyethylene film showed no effect on the resulting IEC of 2.3 mmol g^{-1} for a given value of DOG. This is because as shown in previous section, the use of high VBC concentration enhanced monomer mass transport through LDPE film even at high dose rate of 20 kGy thereby the influence of varying the thickness was not observed. Furthermore, based on the results, the thinnest membrane will be the most desirable due to better water transport and lower resistance. However, this will come at the cost of increase in the gas cross-over (H_2).

The measured IEC (Table 3) is lower than the estimated theoretical value from the DOG values due to the following reasons: incomplete amination of the LDPE-g-VBC copolymer, limitation of accessing all the functional sites and incomplete ion exchange between OH^- and Cl^-. The calculated value of hydration number (λ) is also high of 61 (IEC 2.3 mmol g^{-1}). This is around three times that of fully hydrated Nafion and mainly caused by the high IEC. The IEC of the most prepared membranes in Table 3 are ca. 2.55 times higher than that of Nafion 117 (0.91 mmol g^{-1}). This high IEC and consequently high λ is required to achieve high OH^- ionic conductivities in the order of 0.1 S cm^{-1}. Conductivity of ions is a function of both the ion mobility and the concentration of charge carriers. The ratio of the ion mobility in dilute solution of that of H^+ to OH^- is around 1.77 [1]. Which means that to achieve similar H^+ ionic conductivity in Nafion, AEM should have IEC ca. double that of Nafion to balance the slow diffusion of hydrated OH^- in comparison to that of the hydrated H^+. Moreover, Nafion binds water more strongly than the relatively weak base in AEM, the absorbed water is less bound within the AEM polymer structure because there are not as many ion pairs dissociated [37] and higher IEC is required to stop AEM from dehydration at temperatures above 60 °C. An IEC over 2 mmol g^{-1} is required for AEM to achieve similar effective water self-diffusion coefficients in Nafion of 10^{-9} m^2 s^{-1} at 25 °C [37]. However excessive water uptake will lead to excessive swelling leading to dimensional deformation and structural instability of the membrane. Therefore, a good balance between IEC and WU is desired.

Similar with λ, the water uptake WU is also measure of the amount of water in the membrane in terms of wt% or vol% which results in membrane swelling DS%. Consequently, high DOG, hence high IEC, will lead to high WU and high DS. Since all membranes regardless of initial polyethylene thickness showed essentially constant IEC and DOG at the same grafting conditions (Table 3), expectedly the membranes exhibited the same high value of WU around 255 wt% (IEC 2.3 mmol g^{-1}). While initial look at this value suggests significantly higher number than Nafion WU ca. 30 wt% (Table 4), WU based on wt % has its limitations due to its failure to consider the density of the polymer (Nafion of ca. 2 g cm^{-3} [38] in comparison to LDPE-VBC-TMA of ca. 0.95 g cm^{-3}). More relevant comparison

Table 3 – DOG, IEC, WU, λ, and swelling of membranes with increasing initial LDPE thickness measured at room temperature.

Initial polyethylene film thickness (μm)	Membrane thickness after grafting (μm)	DOG (%)	IEC_{theo} (mmol g^{-1})	Measured IEC (mmol g^{-1})	WU (wt %)	WU (vol %)	λ	Membrane swelling			
								DS_z (%)	DS_x (%)	DS_y (%)	Average (%)
30	49	67.5	3.5	2.3	255	70.8	61.6	57.9	41.5	60.3	53.2
50	63	32.0	1.9	1.4	130	54.8	53.5	30.2	20.8	17.9	23.0
50	75	65.4	3.4	2.3	253	70.6	61.1	53.9	52.5	36.9	47.8
50	95	74.6	3.8	3.2	285	73.1	52.8	58.9	57.1	50.7	55.6
75	96	65.6	3.4	2.3	254	70.7	61.3	49.6	34.6	32.3	38.8
130	169	59.9	3.2	2.3	259	71.0	62.5	51.1	43.1	38.9	44.4

Table 4 – WU, λ and swelling of Nafion membranes having IEC of 0.91 mmol g^{-1}.

Membrane code	Nominal thickness (μm)	WU (wt %)	WU[a] (vol %)	λ[a]	DS (%)	Reference
212	51	30.3[c,1]	37.7	18.5	39.6[b,2]	[1]Takamuku and Jannasch [40] [2]Sherazi et al. [41]
117	183	19.22[d]	27.8	11.7	37.4[d]	Xu et al. [42]

[a] Calculated based on reported WU (wt %) and using Nafion density of 2 g cm^{-3} [38].
[b] Measured at 20 °C.
[c] Measured at room temperature.
[d] Measured at 30 °C.

is to look at the WU in vol% [39]. The WU vol% for AEM with IEC of 2.3 mmol g^{-1} was ca. 70% (Table 3) around 2.5 times that of Nafion (Table 4) which is in agreement with the ratio of IEC and λ.

The WU is also related to the swelling, which can be measured by the increase of membrane thickness or by dimensional expansion due to the water content at room temperature. Higher WU causes higher swelling of the membrane. The membrane exhibited isotropic swelling wherein dimensional change was similar both along the in-plane (width and length) direction and the through-plane (thickness) direction. As expected, average swelling was essentially constant at given IEC and WU of ca. 50% for IEC of 2.3 mmol g^{-1}. As expected, the observed swelling is found to be higher to that exhibited by Nafion membranes as shown in Table 4. The swelling varied with IEC when the measured IEC for LDPE membrane with initial thickness of 50 μm increased from 1.4 to 2.3–3.2 mmol g^{-1}, the DS increased from 23.0 to 47.8–55.6%.

Tensile test

Mechanical testing was performed to determine the effect of swelling and WU on the resulting tensile strength of the hydrated membranes of different DOG. A sample of the initial LDPE film and fully hydrated commercial Nafion 212 film were also tested for comparison wherein the stress-strain curves of all the samples are shown in Fig. 3. As summarised in Table 5, both dry AEMs, 32% and 65% DOG, showed comparable ultimate tensile strength (UTS) of 9.5 and 11.2 MPa, respectively. This indicates that the amount of VBC monomer did not significantly affect the tensile strength of the dry membranes. These values are also slightly lower than that of pristine LDPE film of 15.5 MPa.

Table 5 – Ultimate tensile strength of the test specimens.

Test specimen		Ultimate tensile strength (MPa)
LDPE precursor film		15.5
Fully hydrated Nafion 212 film		9.0
65% DOG	Dry LDPE-AEM	11.2
	Fully hydrated LDPE-AEM	2.4
32% DOG	Dry LDPE-AEM	9.5
	Fully hydrated LDPE-AEM	6.6

Fully hydrated membranes, on the other hand, has as expected significantly lower UTS of 6.6 and 2.4 MPa for AEMs with DOG of 32% and 65%, respectively. The higher the grafting degree (65% – Table 3) the higher the membrane degree of swelling (DS of 48%) and the poorer the mechanical properties, i.e. decrease by 79% of UTS (from 11.2 to 2.4 MPa) compared to AEM with lower DOG (32%) and consequently lower DS (23%) and lower loss of UTS of 30% (from 9.5 to 6.6 MPa).

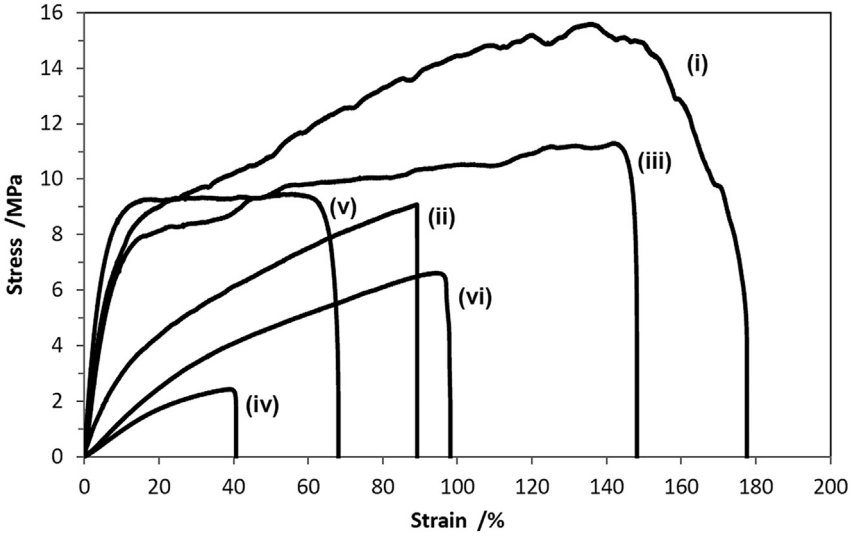

Fig. 3 – Stress–strain curves of the (i) LDPE base film, (ii) fully hydrated Nafion 212 film, (iii) dry LDPE-AEM (65% DOG), (iv) fully hydrated LDPE-AEM (65% DOG), (v) dry LDPE-AEM (32% DOG), and (vi) fully hydrated LDPE-AEM (32% DOG).

The commercial Nafion film exhibited a UTS of 9.0 MPa (Table 5) which is in agreement with values reported in literature [43]. While the AEM with low DOG of 32% has an IEC 1.5 that of Nafion (and lower ionic conductivity), the UTS of the hydrated AEM is lower than that of Nafion by only 26%. Furthermore, when compared with other polymers, the tensile strength of the AEM with the use of LDPE as the base polymer is still inferior compared to that of polytetrafluoroethylene (PTFE) [44] and ethylene tetrafluoroethylene (ETFE) [43] as the base polymers. HDPE and UHMWPE can be used in the future instead of LDPE to improve the mechanical strength of the initial base polymer and consequently the final produced AEM. As mentioned earlier, since the OH^- diffusion is ca. 2 times slower than H^+ in dilute solutions, the authors see the optimum balance between IEC and mechanical properties shifts towards higher IEC values, in comparison to PEM, at the cost of mechanical properties.

Ionic conductivity

The IEC and DOG data from Table 2 are important membrane parameters that can be directly correlated with the measured ionic conductivity. Fig. 4 shows the variation in conductivity of the radiation grafted membranes with temperature as a function of increasing DOG. It can be observed that as the DOG increased, the ionic conductivity also increased. As shown for ENTEK-based porous membrane, an increase from 46.0% to 57.4% DOG exhibited an increase in ionic conductivity at 70 °C from 0.05 to 0.08 S cm^{-1}, respectively. Similarly, BPI-based non-porous membrane showed an increase in ionic conductivity from 0.09 to 0.11 S cm^{-1} at 60 °C when the DOG was increased from 50.4% to 74.6%, respectively.

By comparing relatively similar DOG of membranes from different polyethylene sources, namely VWR-based AEM (51.7% DOG) and BPI-based AEM (50.4% DOG), we can establish that varying the commercial polyethylene supply source has minimal effect on the ionic conductivity of the fabricated AEM. It can be observed that both membranes exhibited essentially the same ionic conductivity at all temperatures tested ruling out the effect of variation in supplier on the properties of the resulting AEM, particularly in terms of ionic conductivity.

ENTEK-based porous membranes were compared with non-porous VWR-based membranes, at similar DOG. The non-porous VWR-based membrane showed superior conductivity compared to the porous ENTEK-based membrane. At 70 °C, the non-porous VWR-based membrane with 51.7% DOG showed higher conductivity of 0.097 S cm^{-1} compared to 0.078 S cm^{-1} exhibited by the porous ENTEK-based membrane with 57.4% DOG. The observed difference in conductivity by ca. 20% is believed to be caused by the remaining porosity in ENTEK membranes after grafting. This porosity led to a very high hydrogen fuel cross-over through the membrane and the recorded OCV was lower than 0.4 V, thus the fuel cell performance data was no longer collected.

Among the different AEMs tested, the VWR-polyethylene based membrane with DOG of 71.3% (IEC 3.0 mmol g^{-1}) showed the highest conductivity of 0.12 S cm^{-1} at 70 °C. This value is much higher compared to similar studies of polyethylene-based AEMs at the same temperature [23]. This makes the fabricated membrane a good candidate for alkaline fuel cell systems being capable of supporting large currents with minimal resistances loss.

Fuel cell performance

Fig. 5 shows the fuel cell polarisation curve for anion-exchange membranes with 74.6% and 32.0% DOG at 40 °C, using air and oxygen feed under atmospheric pressure. Under oxygen feed, the measured OCV were 1.06 and 1.08 V for 74.6% and 32.0% DOG, respectively. The high recorded OCVs indicate that the studied DOG range and the resulting membrane swelling degrees are suitable for fuel cells application with low fuel cross-over across the cell. The DS of AAEM with DOG of 74.6% was ca. 55.6% and the DS of AEM with DOG of 32.0% was 23.0% (Table 3) in comparison to that of Nafion 212 of 40% and Nafion 117 of 37% as shown in Table 4. The use of AEM with increased DOG is beneficial in attaining higher performance of

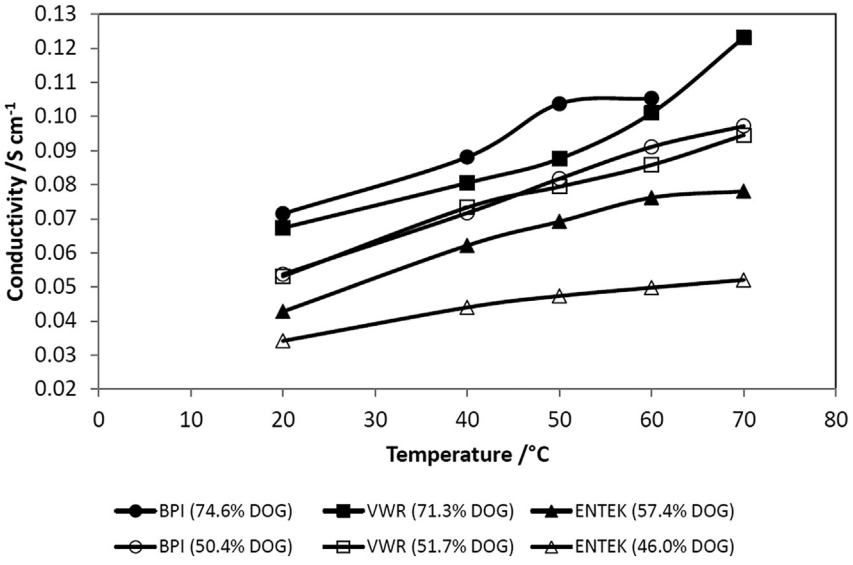

Fig. 4 – Through-plane conductivity of membranes at different temperatures.

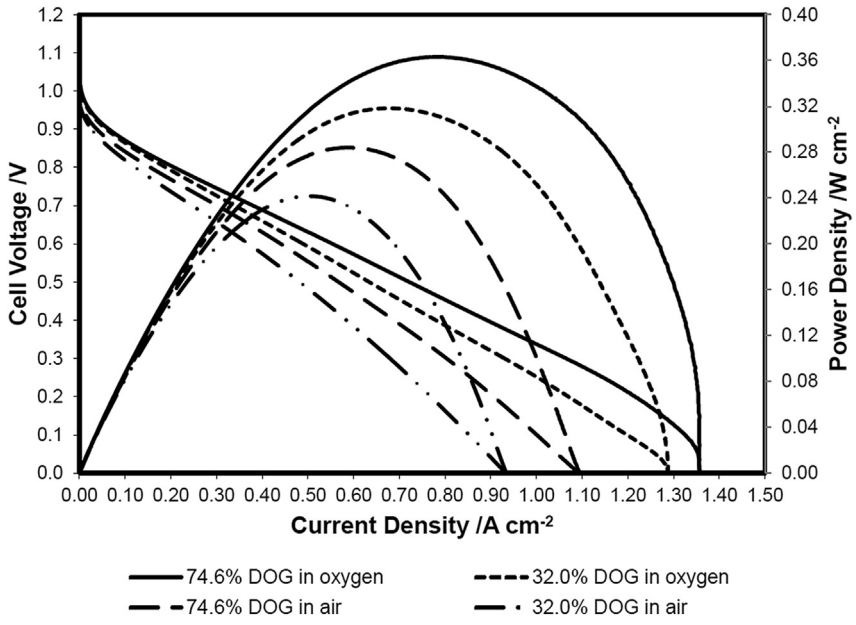

Fig 5 – Polarisation and power density curves of LDPE-based anion exchange membranes at 40 °C both at oxygen and air atmosphere.

the fuel cell due to better conductivity, resilience to dehydration and water transport from anode to cathode. As can be seen in Fig. 5, the slope of the I–V curve improved upon using AAEM with higher DOG due to lower membrane resistivity from 158 mΩ cm^2 for 32.0% DOG to 143 mΩ cm^2 for 74.6% DOG (measured using FRA) resulting in an increase in current density from 502 to 544 mA cm^{-2} at 0.6 V, respectively. The resistivity decrease translates to ionic conductivity increase by a factor of 2 considering the difference in thickness between the two membranes (Table 6). While both polymer films had the same initial thickness of 50 μm, the thickness of the dry film with higher DOG of 74.6% was 1.5 that of the lower DOG of 32.0% after grafting (Table 3). The consequent difference in IEC and WU when hydrated resulted in even larger difference in the final hydrated films thickness by a factor of 1.84 (Table 6).

Data further shows that the difference between oxygen and air performance at 40 °C is rather small indicating good electrode architecture and good hydration level with minimal transfer losses at the cathode. For the membrane having 74.6% DOG, the current density at 0.6 V was 544 mA cm^{-2} under oxygen and 415 mA cm^{-2} under air. The plot shows approximately linear behaviour at medium current densities. While normally this region is referred to as the ohmic region, contribution from mass transport effects are also present [1,22]. This can be seen from the difference in the polarisation slopes between air and oxygen operation.

Table 6 – MEAs through plane resistivity at 40 °C under oxygen with different DOG and corresponding membrane thickness.

Membrane DOG (%)	Initial PE thickness (μm)	Hydrated thickness (μm)	FRA through-plane resistance (mΩ cm^2)
32.0	50	82	158
74.6	50	151	143

Fig. 6 shows the fuel cell polarisation curve for anion-exchange membranes with 74.6% and 32.0% DOG at 50 °C, both using air and oxygen feed under atmospheric pressure. It can be seen that for the membrane electrode assembly (MEA) utilising 74.6% DOG membrane under oxygen feed, the obtained current density at 0.6 V was 643 mA cm^{-2}, higher compared to that at 40 °C of 544 mA cm^{-2}. Similarly, for the MEA with 32.0% DOG membrane, the current density at 0.6 V under oxygen increased from 502 to 546 mA cm^{-2} when the working temperature was increased from 40 to 50 °C, respectively. Despite the observed increase in current density under oxygen with temperature, the dehydration of MEA with 32.0% DOG membrane became evident at a closer look. A clear mass transport limitation represented by a limiting current even under oxygen operation at ca. 1.2 A cm^{-2} was observed (Fig. 6, 32.0% DOG). This is an indication of membrane/ionomer dehydration and consequently decrease in oxygen permeability (through ionomer) and water permeability (through ionomer and membrane) both of which are reactants at the cathode. This is also supported by the resistivity measurements where the through plane resistivity of MEA utilising membrane with 32.0% DOG increased from 158 to 199 Ω cm^2 (Table 7). The dehydration effect became more apparent under air operation where higher flow rates are used at the cathode. The current density under air at 0.6 V decreased (32.0% DOG) from 372 to 342 mA cm^{-2} with temperature increase from 40 to 50 °C, respectively.

On the other hand, MEA utilising membrane with 74.6% DOG did not suffer dehydration at 50 °C under oxygen. This can be seen by no clear limiting current even at current density of 2.2 A cm^{-2} under oxygen. This was additionally confirmed by decrease in the measured resistivity from 143 to 122 with temperature increase from 40 to 50 °C, respectively.

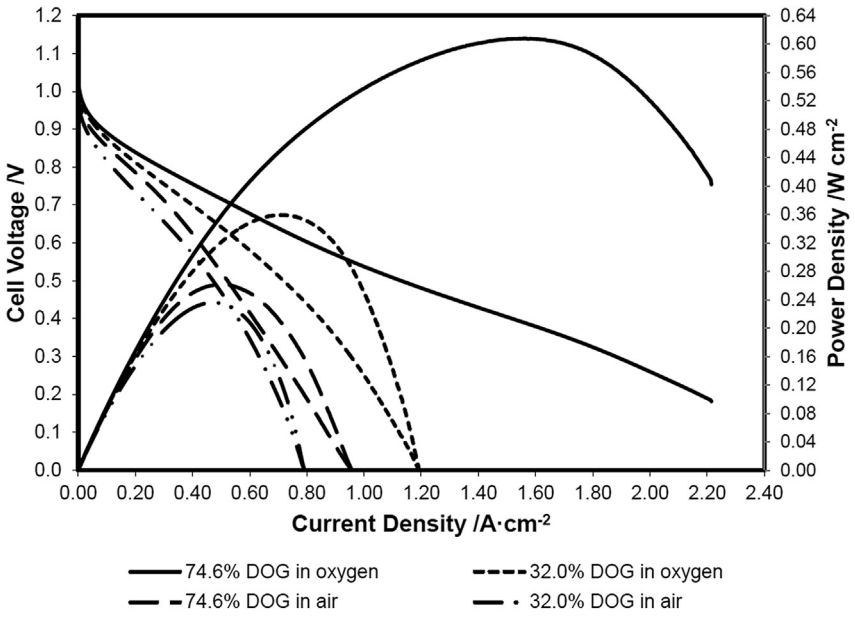

Fig. 6 – Polarisation and power density curves of LDPE-based anion exchange membranes at 50 °C both at oxygen and air atmosphere.

Table 7 – MEAs through plane resistivity at 50 °C under oxygen with different DOG.

Membrane DOG (%)	FRA through-plane resistance (mΩ cm^2)
32.0	199
74.6	122

The measured WU of the 32.0% DOG membrane was 130 wt %, considerably lower compared to 285 wt% for the 74.6% DOG membrane (at RT) explaining the observed dehydration limitation in the case of 32.0% DOG membrane. It can be therefore reiterated that in order to operate AEM for prolonged periods at temperatures of 50 °C and above, the use of membranes with high DOG is required.

Peak power density and current density values at 0.6 V are summarised in Table 8. Under oxygen gas feed at 50 °C, the membrane with 74.6% DOG exhibited peak power density and current density at 0.6 V of 608 mW cm^{-2} and 643 mA cm^{-2}, respectively. On the other hand, using air as the feed showed peak power density and current density at 0.6 V of 262 mW cm^{-2} and 461 mA cm^{-2}, respectively. Similarly for the 32.0% DOG membrane, the peak power density and current density at 0.6 V at 50 °C under oxygen were 359 mW cm^{-2} and 546 mA cm^{-2}, respectively, while under air were 236 mW cm^{-2} and 342 mA cm^{-2}, respectively.

Membrane stability

Stability of the LDPE-g-VBC membrane (71.3% DOG) was investigated in terms of ionic conductivity in vapour phase condition for a total of 29 weeks. The test was performed with a stepwise increase in temperature from 40 to 80 °C wherein a stable conductivity reading was obtained for few weeks before shifting to the higher temperature. The plot of membrane conductivity for different temperature regime is shown in Fig. 7. The observed fluctuations in the conductivity data at 80 °C were due to regular replenishment of deionised water into the humidifier.

Expectedly, the conductivity of the membrane increased with increasing cell temperature from 0.06 to 0.11 S cm^{-1} peak conductivity. At the highest temperature of 80 °C, the conductivity was extremely stable at average ca. 0.11 S cm^{-1} for a 12-week continuous run under nitrogen with a degradation

Table 8 – Summary of peak power density and current density at 0.6 V of the fabricated membranes.

DOG (%)	Temperature (°C)	Gas feed	Peak power density (mW cm^{-2})	Current density at 0.6 V (mA cm^{-2})
74.6	40	Oxygen	363.3	543.5
		Air	284.0	414.6
	50	Oxygen	607.8	643.0
		Air	261.6	460.6
32.0	40	Oxygen	318.5	502.3
		Air	241.7	372.2
	50	Oxygen	359.3	546.0
		Air	235.9	342.4

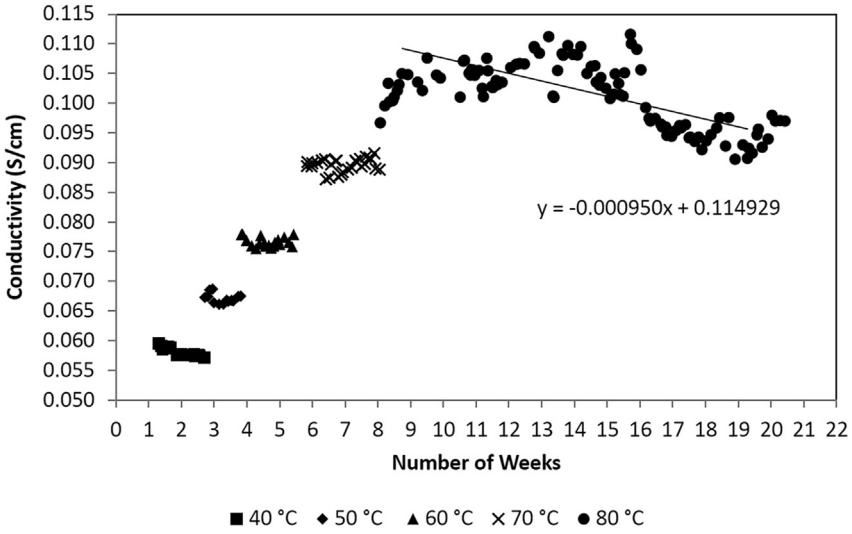

Fig. 7 – Through-plane conductivity of LDPE-g-VBC membrane (71.3% DOG) with increasing temperature under nitrogen.

rate of 4 mS month^{-1}. At a conductivity cut-off point of 0.02 S cm^{-1} for the membrane, the estimated life time under nitrogen would be 2 years. This demonstrated that the produced membrane exhibited superb stability considering the fact that the membrane was subjected to an extremely harsh test temperature of 80 °C. Typical alkaline fuel cells usually do not operate above 50 °C because of dehydration which results in faster degradation [45]. Thus it is expected that the calculated life time of the produced membrane will be significantly longer at 50 °C.

After obtaining a stable conductivity of the membrane for 20 weeks, the gas feed was changed to oxygen to determine its effect on membrane stability. A closer look on the data shown in Fig. 8, it can be seen that the conductivity gradually and continuously decreased from around 0.10 to 0.07 S cm^{-1} in 6 weeks resulting in an average degradation rate of 17 mS month^{-1}. At a conductivity cut-off point of 0.02 S cm^{-1} for the membrane, the estimated life time under oxygen would be 5.5 months operating under 80 °C.

The observed degradation due to oxidation of functional group and backbone is subject to further investigation and will be reported in detail in future publication. After the 6 week period, the gas feed was reverted to nitrogen to check whether the conductivity decline of the membrane will stop. It can be observed from Fig. 8 that the decrease in conductivity was abated but the membrane did not recover its original high conductivity. It can be concluded that membrane degradation caused by oxidation was permanent.

Conclusion

The fabrication of polyethylene-based alkaline anion-exchange membrane was successfully performed by mutual

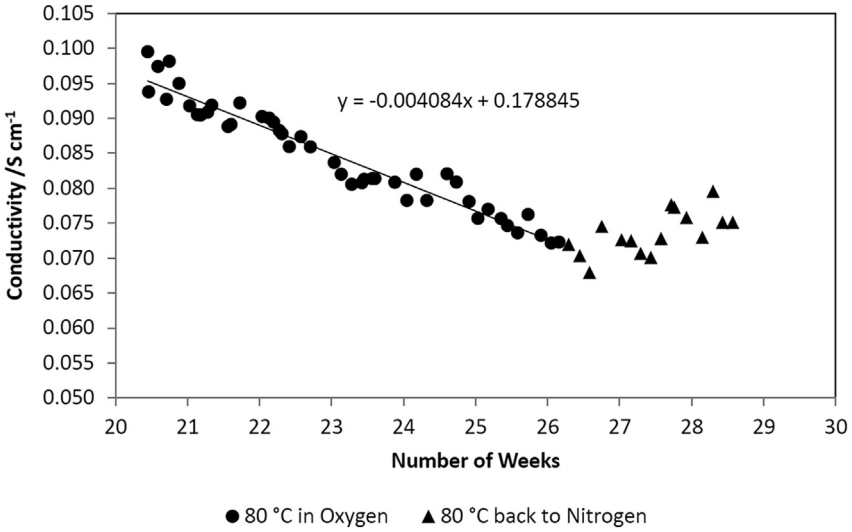

Fig. 8 – Degradation of LDPE-g-VBC membrane (71.3% DOG) under oxygen gas feed at 80 °C.

radiation graft polymerisation with the use of both laboratory-cast and commercially procured polyethylene film. Anion-exchange membrane conductivity increased with VBC concentration and gamma radiation dose. Cast-LDPE membrane showed higher DOG than cast-LLDPE membrane at low VBC concentration due to the absence of chain branching in LLDPE. The variation in suppliers of commercial polyethylene had insignificant effect on the ionic conductivity of the fabricated AEMs. The use of porous ENTEK polyethylene as base polymer film resulted in higher DOG compared to non-porous LDPE at the same grafting conditions due to the ease with which the VBC monomer can penetrate the porous structure of the base polymer. However, the AEM remained porous over 5% after radiation grafting rendering it not useful for fuel cell applications. Mechanical testing revealed that when fully hydrated, the AEM ultimate tensile strength (UTS) is significantly reduced with increase in DOG and consequent increase in swelling. At 32% DOG, the value was 26% lower than Nafion UTS. However, due to slower OH^- diffusion (ca. 2 times) in comparison to H^+, the optimum balance between conductivity and mechanical strength shifts towards higher IEC values, in comparison to PEM, at the cost of mechanical properties.

The observed ionic conductivity and the IEC increased with increase in DOG wherein VWR-based AEM with 71.3% DOG exhibited the highest conductivity of 0.12 S cm^{-1} at temperature of 70 °C among the membranes prepared with 50 μm initial LDPE thickness. The initial thickness of the polyethylene film was found to have no influence on the resulting IEC and DOG of the produced membrane. Similarly, the WU and swelling were essentially constant at fixed DOG regardless of the initial polyethylene thickness. To achieve similar H^+ ionic conductivity in Nafion (0.1 S cm^{-1} at 80 °C, 100% RH), AEM should have IEC > 2.0 mmol g^{-1} double that of Nafion to balance the slow diffusion of hydrated OH^- in comparison to that of the hydrated H^+. Moreover, Nafion binds water more strongly than the relatively weak base in AEM, and higher IEC is required to stop AEM from dehydration at temperatures above 60 °C.

Membrane electrode assembly based on fabricated AEM showed high OCVs of 1.06 and 1.08 V for 32.0% and 74.6% DOG membranes, respectively. This shows that membranes with DOG <75% are suitable for fuel cell application with low fuel cross-over. Furthermore, the use of membrane with high DOG provided improved fuel cell performance due to better ionic conductivity and water transport from anode to cathode. Polarisation curves showed that the fuel cell performance can be improved by increasing the operating temperature from 40 to 50 °C. The best performing AEM with hydrated thickness of 151 μm (74.6% DOG) achieved peak power density of 608 mW cm^{-2} and maximum current density at 0.6 V of 643 mA cm^{-2} under oxygen at 50 °C. In order to operate AEM for prolonged periods at temperatures of 50 °C and above, the use of membranes with high DOG >32% is required.

The LDPE-based membrane (71.3% DOG) was subjected to stability test for 29 weeks and was found to be extremely stable at temperature of up to 80 °C for 12 weeks under nitrogen, with average conductivity of 0.11 S cm^{-1} and degradation rate of 4 mS $month^{-1}$. However, the membrane continuously lost conductivity when exposed to oxygen gas at 80 °C with a degradation rate of 17 mS $month^{-1}$. At a conductivity cut-off point of 0.02 S cm^{-1}, the membrane projected life time under nitrogen is 2 years and 5.5 months under oxygen operating under 80 °C. The life time of the prepared membrane will however be significantly longer when it is operated at a lower temperature of typically 50 °C.

Acknowledgement

The authors acknowledge the support of the Engineering and Physical Sciences Research Council (EPSRC-UK) for funding under grant number EP/M005933/1 and the Philippine Department of Science and Technology through the Engineering Research for Development and Technology Program (ERDT-DOST) for funding Richard Espiritu's PhD fellowship. The authors further express their gratitude to Dr. Prodip Das of the School of Mechanical and Systems Engineering, Newcastle University for the assistance in mechanical testing of the membranes.

REFERENCES

[1] Mamlouk M, Scott K. Effect of anion functional groups on the conductivity and performance of anion exchange polymer membrane fuel cells. J Power Sources 2012;211:140–6.
[2] Mamlouk M, Wang X, Scott K, Horsfall JA, Williams C. Characterization and application of anion exchange polymer membranes with non-platinum group metals for fuel cells. Proc Inst Mech Eng Part A J Power Energy 2011;225:152–60.
[3] Park J-S, Park S-H, Yim S-D, Yoon Y-G, Lee W-Y, Kim C-S. Performance of solid alkaline fuel cells employing anion-exchange membranes. J Power Sources 2008;178:620–6.
[4] Arges CG, Ramani V, Pintauro PN. Anion exchange membrane fuel cells. Electrochem Soc Interface 2010;19:31–5.
[5] Cao Y-C, Wang X, Scott K. The synthesis and characteristic of an anion conductive polymer membrane for alkaline anion exchange fuel cells. J Power Sources 2012;201:226–30.
[6] Varcoe JR, Slade RCT. Prospects for alkaline anion-exchange membranes in low temperature fuel cells. Fuel Cells 2005;5:187–200.
[7] Wang X, Li M, Golding BT, Sadeghi M, Cao Y, Yu EH, et al. A polytetrafluoroethylene-quaternary 1,4-diazabicyclo-[2.2.2]-octane polysulfone composite membrane for alkaline anion exchange membrane fuel cells. Int J Hydrogen Energy 2011;36:10022–6.
[8] Couture G, Alaaeddine A, Boschet F, Ameduri B. Polymeric materials as anion-exchange membranes for alkaline fuel cells. Prog Polym Sci 2011;36:1521–57.
[9] Nasef MM. Fuel cell membranes by radiation-induced graft copolymerization: current status, challenges, and future directions. In: Zaidi SMJ, Matsuura T, editors. Polymer membranes for fuel cells. Springer US; 2009. p. 87–114.
[10] Franjo Ranogajec MM, Hell Zvonimir. Improvement of the polymer properties by radiation grafting and crosslinking. Polimeri 2008;29:236–43.
[11] Dargaville TR, George GA, Hill DJT, Whittaker AK. High energy radiation grafting of fluoropolymers. Prog Polym Sci 2003;28:1355–76.
[12] Tamboli SM, Mhaske ST, Kale DD. Crosslinked polyethylene. Indian J Chem Technol 2004;11:853–64.

[13] Horsfall JA, Lovell KV. Fuel cell performance of radiation grafted sulphonic acid membranes. Fuel Cells 2001;1:186–91.
[14] Alkan Gürsel S, Gubler L, Gupta B, Scherer G. Radiation grafted membranes. In: Scherer G, editor. Fuel cells I. Springer Berlin Heidelberg; 2008. p. 157–217.
[15] Nasef MM, Hegazy E-SA. Preparation and applications of ion exchange membranes by radiation-induced graft copolymerization of polar monomers onto non-polar films. Prog Polym Sci 2004;29:499–561.
[16] Zhang M, Kim HK, Chalkova E, Mark F, Lvov SN, Chung TCM. New polyethylene based anion exchange membranes (PE–AEMs) with high ionic conductivity. Macromolecules 2011;44:5937–46.
[17] Kim HK, Zhang M, Yuan X, Lvov SN, Chung TCM. Synthesis of polyethylene-based proton exchange membranes containing PE backbone and sulfonated Poly(arylene ether sulfone) side chains for fuel cell applications. Macromolecules 2012;45:2460–70.
[18] Nasef MM. Radiation-grafted membranes for polymer electrolyte fuel cells: current trends and future directions. Chem Rev 2014;114:12278–329.
[19] Masson JP, Molina R, Roth E, Gaussens G, Lemaire F. Obtention and evaluation of polyethylene-based solid polymer electrolyte membranes for hydrogen production. Int J Hydrogen Energy 1982;7:167–71.
[20] Faraj M, Boccia M, Miller H, Martini F, Borsacchi S, Geppi M, et al. New LDPE based anion-exchange membranes for alkaline solid polymeric electrolyte water electrolysis. Int J Hydrogen Energy 2012;37:14992–5002.
[21] Mamlouk M, Horsfall JA, Williams C, Scott K. Radiation grafted membranes for superior anion exchange polymer membrane fuel cells performance. Int J Hydrogen Energy 2012;37:11912–20.
[22] Mamlouk M, Scott K, Horsfall JA, Williams C. The effect of electrode parameters on the performance of anion exchange polymer membrane fuel cells. Int J Hydrogen Energy 2011;36:7191–8.
[23] Sherazi TA, Yong Sohn J, Moo Lee Y, Guiver MD. Polyethylene-based radiation grafted anion-exchange membranes for alkaline fuel cells. J Membr Sci 2013;441:148–57.
[24] Shen M, Roy S, Kuhlmann J, Scott K, Lovell K, Horsfall J. Grafted polymer electrolyte membrane for direct methanol fuel cells. J Membr Sci 2005;251:121–30.
[25] Cheng H, Scott K, Lovell KV, Horsfall JA, Waring SC. Evaluation of new ion exchange membranes for direct borohydride fuel cells. J Membr Sci 2007;288:168–74.
[26] Noonan KJT, Hugar KM, Kostalik HA, Lobkovsky EB, Abruña HD, Coates GW. Phosphonium-functionalized polyethylene: a new class of base-stable alkaline anion exchange membranes. J Am Chem Soc 2012;134:18161–4.
[27] Zhao Y, Yu H, Xie F, Liu Y, Shao Z, Yi B. High durability and hydroxide ion conducting pore-filled anion exchange membranes for alkaline fuel cell applications. J Power Sources 2014;269:1–6.
[28] Gruzd AS, Trofimchuk ES, Nikonorova NI, Nesterova EA, Meshkov IB, Gallyamov MO, et al. Novel polyolefin/silicon dioxide/H3PO4 composite membranes with spatially heterogeneous structure for phosphoric acid fuel cell. Int J Hydrogen Energy 2013;38:4132–43.
[29] Scott K, Mamlouk M, Espiritu R, Wu X. Progress in alkaline membrane fuel cells and regenerative fuel cells. ECS Trans 2013;58:1903–6.
[30] Jikihara A, Ohashi R, Kakihana Y, Higa M, Kobayashi K. Electrodialytic transport properties of anion-exchange membranes prepared from Poly(vinyl alcohol) and Poly(vinyl alcohol-co-methacryloyl aminopropyl trimethyl ammonium chloride). Membranes 2013;3:1.
[31] Horsfall JA, Lovell KV. Synthesis and characterisation of sulfonic acid-containing ion exchange membranes based on hydrocarbon and fluorocarbon polymers. Eur Polym J 2002;38:1671–82.
[32] Gulmine JV, Janissek PR, Heise HM, Akcelrud L. Polyethylene characterization by FTIR. Polym Test 2002;21:557–63.
[33] Moez AA, Aly SS, Elshaer YH. Effect of gamma radiation on low density polyethylene (LDPE) films: optical, dielectric and FTIR studies. Spectrochim Acta Part A Mol Biomol Spectrosc 2012;93:203–7.
[34] Yoko K. Effects of gamma irradiation on polyethylene, polypropylene, and polystyrene. Irradiation of food and packaging. American Chemical Society; 2004. p. 262–76.
[35] Krasnansky VJ, Achhammer BG, Parker MS. Effect of gamma radiation on chemical structure of plastics. Polym Eng Sci 1961;1:133–8.
[36] Liu H, Yang S, Wang S, Fang J, Jiang L, Sun G. Preparation and characterization of radiation-grafted poly (tetrafluoroethylene-co-perfluoropropyl vinyl ether) membranes for alkaline anion-exchange membrane fuel cells. J Membr Sci 2011;369:277–83.
[37] Hibbs MR, Hickner MA, Alam TM, McIntyre SK, Fujimoto CH, Cornelius CJ. Transport properties of hydroxide and proton conducting membranes. Chem Mater 2008;20:2566–73.
[38] Zook LA, Leddy J. Density and solubility of nafion: recast, annealed, and commercial films. Anal Chem 1996;68:3793–6.
[39] Kim YS, Pivovar BS. Moving beyond mass-based parameters for conductivity analysis of sulfonated polymers. Annu Rev Chem Biomol Eng 2010;1:123–48.
[40] Takamuku S, Jannasch P. Properties and degradation of hydrocarbon fuel cell membranes: a comparative study of sulfonated poly(arylene ether sulfone)s with different positions of the acid groups. Polym Chem 2012;3:1202–14.
[41] Sherazi TA, Zahoor S, Raza R, Shaikh AJ, Naqvi SAR, Abbas G, et al. Guanidine functionalized radiation induced grafted anion-exchange membranes for solid alkaline fuel cells. Int J Hydrogen Energy 2015;40:786–96.
[42] Yu Xu P, Zhou K, Lu Han G, Gen Zhang Q, Mei Zhu A, Lin Liu Q. Fluorene-containing poly(arylene ether sulfone)s as anion exchange membranes for alkaline fuel cells. J Membr Sci 2014;457:29–38.
[43] Varcoe JR, Slade RCT, Lam How Yee E, Poynton SD, Driscoll DJ, Apperley DC. Poly(ethylene-co-tetrafluoroethylene)-Derived radiation-grafted anion-exchange membrane with properties specifically tailored for application in metal-cation-free alkaline polymer electrolyte fuel cells. Chem Mater 2007;19:2686–93.
[44] Cao Y-C, Scott K, Wang X. Preparation of polytetrafluoroethylene porous membrane based composite alkaline exchange membrane with improved tensile strength and its fuel cell test. Int J Hydrogen Energy 2012;37:12688–93.
[45] Varcoe JR, Poyton DS, Slade RCT. Chapter 21: Alkaline anion-exchange membranes for low-temperature fuel cell application. In: Vielstich W, Gasteiger HA, Yokokawa H, editors. Handbook of fuel cells. Advances in electrocatalysis, materials, diagnostics and durability, vol. 5. John Wiley Sons, Ltd.; 2009. p. 322–33.